

DRUG-LOADED MESOPOROUS SILICA/CALCIUM PHOSPHATE COMPOSITES FOR BONE REGENERATION

ADRIAN SZEWCZYK, ADRIANNA SKWIRA,
MAGDALENA PROKOPOWICZ*

DEPARTMENT OF PHYSICAL CHEMISTRY,
FACULTY OF PHARMACY, MEDICAL UNIVERSITY OF GDAŃSK,
HALLERA 107, 80-416 GDAŃSK, POLAND

*E-MAIL: MAGDALENA.PROKOPOWICZ@GUMED.EDU.PL

Abstract

*In this work, we obtained a mesoporous silica-calcium phosphate composite (MSi-CaP) in the form of spherical granules (pellets) loaded with cefazolin as a model antibiotic. First, the MSi-CaP composite was manufactured in the powder form via the sol-gel method using a soft template. The cefazolin was loaded into the MSi-CaP using the immersion method. The pellets were composed of MSi-CaP powders (both placebo and cefazolin-loaded) and excipients, such as microcrystalline cellulose and ethyl cellulose. The pellets were obtained in the laboratory scale using the wet-granulation, extrusion and spheronization method. The pellets proved satisfactory mechanical properties which allowed for further investigations (the drug release studies and the mineralization potential assay) without a risk of pellets cracking. The complete drug release from the pellets was observed after 12 h. The burst release of cefazolin from the pellets was reduced by 3 when compared to the burst release of cefazolin-loaded MSi-CaP powders (90 and 30% after 15 min of release studies, respectively). The pellets showed the mineralization potential *in vitro*, confirmed by the SEM-EDX and FTIR methods. After 60 days of the mineralization potential assay in the simulated body fluid, the examinations revealed that the whole surface of pellets was covered with the carbonated hydroxyapatite in accordance with the desired morphology.*

Keywords: mesoporous silica, calcium phosphate, hydroxyapatite, composites, drug delivery

[*Engineering of Biomaterials* 150 (2019) 16-21]

Article presented at conference: IMPLANTS 2019,
28-29 June, Gdansk, Poland.

Introduction

Bacterial bone infections occur mainly in adults, usually secondary to open bone injuries, bone reconstructions or implant insertions, and thus are difficult to diagnose and treat [1,2]. Pathogenic changes and necrosis of bone tissue caused by a progressive bacterial infection can be observed via X-ray radiography only if 50-75% of a bone matrix has already been damaged [3]. In most cases a bone biopsy must be performed. In clinical practice, chronic bone inflammation caused by bacterial infection is treated surgically with the simultaneous implementation of antibiotic therapy [2,4]. The use of drug-loaded bone delivery systems (bone fillers) is intended to replace dead tissue, reduce the risk of secondary infection and support bone regeneration [5,6].

Despite advances in surgery, biomaterials engineering, and pharmaceutical technology, bacterial bone infections can remain latent for many years after the treatment, with complete recurrence in 20-30% of patients.

For the last 20 years, bone regenerative medicine has been a promising multidisciplinary science which focuses on biomaterials for bone healing and replacement [5,7]. One of the most innovative strategies for treating bacterial bone infections is the application of bifunctional biomaterials which assure the drug delivery directly into the infected area and support bone regeneration. Much attention is paid to biomaterials which support the damaged bone tissue thanks to the efficient mechanical and biological properties. Among them, mesoporous silica-calcium phosphate composites are investigated [8,9]. Mesoporous silicas are characterized by the high surface area, uniform pore size (4-10 nm), high surface area to volume ratio, modifiable particles shape, and high thermal resistance. Due to these properties, they are studied as drug carriers [10,11]. On the other hand, calcium phosphates, especially hydroxyapatite, are known as excellent bone regenerating biomaterials due to their high biocompatibility and osteoconductivity [12,13]. The calcium phosphates exhibit good biological stability and affinity to bone as they convert into the carbonated hydroxyapatite after implantation. In terms of the composition and structure, the carbonated hydroxyapatite is equivalent to the mineral bone matrix [13,14].

Unfortunately, due to the small particle size of mesoporous silica/calcium phosphate composites, their porosity, low bulk density and adhesion, these materials cannot be directly manufactured in the pharmaceutical technology and biomaterials engineering processes. Only the addition of excipients, the use of appropriate equipment and the proper validation of the manufacturing process makes it possible to obtain a bifunctional drug delivery system for bone regeneration based on mesoporous silica/calcium phosphate composites.

In this work, we obtained the mesoporous silica/calcium phosphate composites formed as pellets loaded with cefazolin as a model antibiotic used to treat bacterial bone infections. The term "pellets" refers to small (approx. 1 mm), free-flowing, spherical granules manufactured by the agglomeration of fine powders via the wet-granulation, extrusion, and spheronization process. The obtained pellets were subjected to the mechanical properties examinations (hardness test, friability test), drug release studies and mineralization potential *in vitro* defined as a possibility to form the hydroxyapatite layer on the surface of the pellets immersed in the simulated body fluid.

Materials and Methods

The mesoporous silica/calcium phosphate composites (MSi-CaP) were synthesized using the sol-gel method [15]. The tetraethyl orthosilicate (TEOS) and cetyltrimethylammonium bromide (CTAB) were used as a silica precursor and a structure directing agent, respectively. The calcium chloride anhydrous (CaCl_2) and potassium dihydrogen phosphate (KH_2PO_4) were applied as calcium phosphate precursors. All reagents were purchased from Sigma-Aldrich. The synthesis was carried out in an aqueous media with the addition of absolute ethanol and 25 wt% ammonia. The corresponding molar ratio of reagents TEOS:CTAB: CaCl_2 : KH_2PO_4 :water:ethanol:ammonia was 0.034:0.007:0.009:0.007:7.33:0.27:0.14. Briefly, water, ethanol, aqueous ammonia and CTAB were mixed in a polypropylene beaker for 15 min, at 300 rpm. The pH of the obtained solution was 10. Next, CaCl_2 , K_2HPO_4 , and TEOS were added and the resulting mixture was continuously stirred for 2 h.

Then the mixture was stored at 90°C for 5 days. The resulting solid product was recovered by the vacuum filtration, washed with 100 ml of absolute ethanol and dried at 40°C for 1 h. The CTAB template was removed from the product using calcination in the air (6 h at 550°C, heating rate of 1°C/min) in a muffle furnace (FCF 7MS series). The final powder composites were micronized in a grinder (Mortar Grinder Pulverisette 2, Fritsch) for 5 min at 75 rpm to obtain 200-500 µm fraction for further studies.

Cefazolin (Cef) was loaded into the composites using the immersion method. In brief, each sample of 200 mg of synthesized composites was immersed for 30 min in a concentrated (10 mg/mL) aqueous solution of cefazolin sodium (Biofazolin, Polpharma) while vigorously shaken. Next, the suspension was filtrated in a vacuum and the concentration of the cefazolin remaining in the solution was examined by monitoring the changes in absorbance at 271 nm by means of the UV-Vis spectrophotometer Shimadzu, (model UV-1800). The cefazolin-loaded composites were dried at room temperature for 24 h. The calculated mean amount of drug loaded into the composite was 32.9 ± 2.5 mg per 1 g of the composite.

Both the placebo mesoporous silica/calcium phosphate composites (MSi-CaP) and the ones loaded with cefazolin (MSi-CaP-Cef) were used to manufacture pellets via the granulation, extrusion and spheronization technique using Caleva Multi Lab apparatus (FIG. 1). The size of each batch was 5 g. Each formulation was composed of MSi-CaP, MSi-CaP-Cef and excipients: microcrystalline cellulose (MCC; Avicel PH 101, Sigma-Aldrich) and ethylcellulose (EC; Ethocel 20 cP, Dow Chemical) in the amounts of 30, 20, 45, 5 wt%, respectively. The powders were first premixed in a mortar and then in a granulator attachment (100 rpm, 5 min). The mass was wet-agglomerated using the EC ethanolic binder solution (5 wt%) in the same attachment (100 rpm, 5 min). The optimal volume of binder solution was determined using Caleva Torque Rheometer. The wet mass was then extruded in an extruder attachment running at 100 rpm with a circular 1 mm holes diameter and depth.

The entire batch of the extrudate was then spheronized in a spheronizer attachment of 8.5 cm in diameter (2500 rpm, 5 min). The resultant pellets were left to dry overnight at room temperature. For further studies (drug release and mineralization potential studies) the main fraction of pellets (0.8-1.0 mm) was chosen as the fraction obtained from sieving with the highest weight (≥80%).

The drug release studies were performed using USP II Paddle Apparatus (Copley DIS-6000) at 37°C, 50 rpm. A constant fraction of the pellets was used for each batch. Purified water (pH=7.0; 500 mL) was applied as a dissolution media providing sink conditions. At suitable time intervals, 2.0 mL of solutions were filtered using membrane filters (0.45 µm) and analyzed spectrophotometrically at 271 nm. The drug stability was provided during the whole release studies. The drug release data were plotted as the cumulative percent of Cef released (Q) as a function of time (t). The release studies were repeated 6 times. The same release studies were carried out for the parent MSi-CaP-Cef powders for comparative purposes.

The mineralization potential assay of the pellets was carried out in the simulated body fluid (SBF) [16]. Each 200 mg of pellets was soaked in 100 mL of SBF in polypropylene containers. The samples were stored in a water bath for 60 days (37°C, 70 rpm). The SBF was exchanged for the fresh one every 24 h.

The composites were investigated using Fourier Transform Infrared Spectroscopy (FTIR, Jasco model 410, KBr technique, 4 cm⁻¹ resolution with spectra standardization to maximum absorbance at ~1080 cm⁻¹ peak), the scanning electron microscopy equipped with energy dispersive X-ray spectroscopy (SEM-EDX, Hitachi SU-70, samples were gold-coated), transmission electron microscopy (TEM, Tecnai G2 T20 X-TWIN) and stereoscopic microscope (Opta-TECH X 2000). The hardness (referred to as a force at 90% strain) and friability of the pellets were tested using texture analyzer (TA.XT plus, granule compaction rig) and friabilator (Erweka TAR 10, 4 min, 25 rpm), respectively.

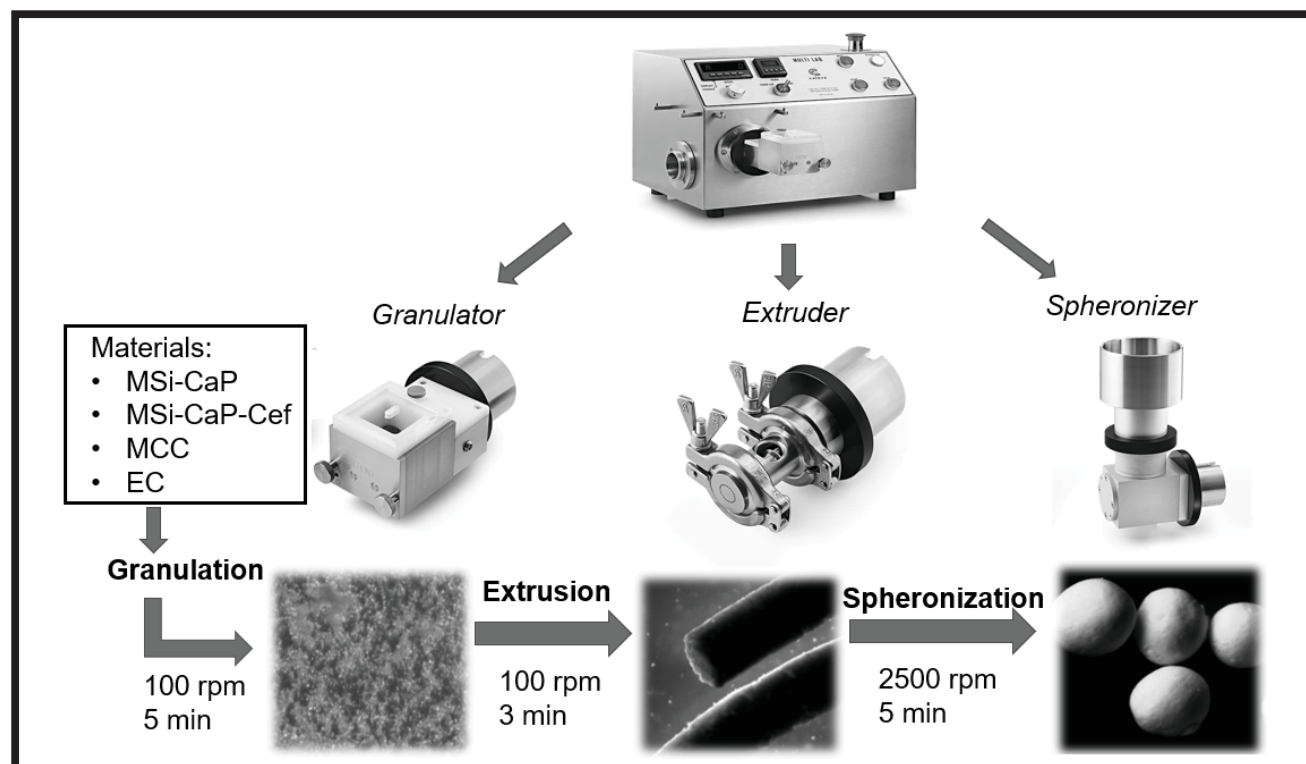


FIG. 1. The schematic illustration of pelletization process for the mesoporous silica-calcium phosphate composites.

Results and Discussions

The SEM and TEM micrographs of MSi-CaP-Cef composite are presented in FIG. 2. Both the SEM (FIG. 2a) and TEM (FIG. 2b) results showed the biphasic nature of the obtained composites: spherical drug-loaded silica particles and rod-like calcium phosphate precipitates. As presented in FIG. 2c, the silica particles were characterized by mesoporous structure (~ 3.5 nm pore diameter), typical for silica materials obtained via the sol-gel method with CTAB as a structure directing agent [17,18].

The FTIR spectra of both the parent and Cef-loaded MSi-CaP powders and pellets are presented in FIG. 3. In the FTIR spectrum of parent MSi-CaP composite (FIG. 3, left) the bands characteristic for silica (1090 , 960 , 800 , 465 cm^{-1} of ν_{as} Si-O-Si; ν_{β} Si-OH; ν_s Si-O and δ O-Si-O vibrational modes, repetitively) [19] and phosphates (604 , 565 cm^{-1} assigned to ν_4 vibrational mode of P-O-P in $(\text{PO}_4)^{3-}$ group) [20] were observed, which also confirmed the biphasic nature of synthesized material. In the case of Cef-loaded composite (MSi-CaP-Cef) (FIG. 3, left) the bands characteristic for Cef molecule confirmed the drug presence in the MSi-CaP composite after the loading procedure. The shift in bands from 1759 to 1761 cm^{-1} and from 1357 to 1363 cm^{-1} may suggest the weak chemical interaction via hydrogen bonding between Cef molecules and the MSi-CaP surface.

The chemical interactions between silanols present on the silica surface and Cef molecules are a well-known phenomenon [21]. It has been reported that the silanols present on the mesoporous silica surface are characterized by pKa approx. 8 and 2 for geminal (Q_2 , $=\text{Si}(\text{OH})_2$) and free (Q_3 , $\equiv\text{SiOH}$) silanols, respectively [22]. Under the provided adsorption conditions (10 mg/mL cefazolin sodium aqueous solution, pH=4.5, room temperature) both CEF molecules and free silanols ($\equiv\text{SiOH} \rightleftharpoons \text{SiO}^- + \text{H}^+$) were negatively charged, whereas the geminal silanols were un-dissociated. Thus, the electrostatic repulsion and hydrogen bonding between silica surface and CEF might influence the adsorption process. However, it is worth mentioning that the adsorption of CEF onto the mesoporous silica was primarily characterized as physical in nature [21]. The FTIR spectrum of final MSi-CaP-Cef pellet (FIG. 3, right) reveals bands characteristic for Cef-loaded MSi-CaP composite (1762 , 1083 , 800 , 604 , 562 , 463 cm^{-1}) and excipients used in pelletization process: microcrystalline cellulose and ethyl cellulose (2975, 2903, 1376, 660 cm^{-1} of C-H stretching, C-H bending and C-OH bending vibrations, respectively) [23].

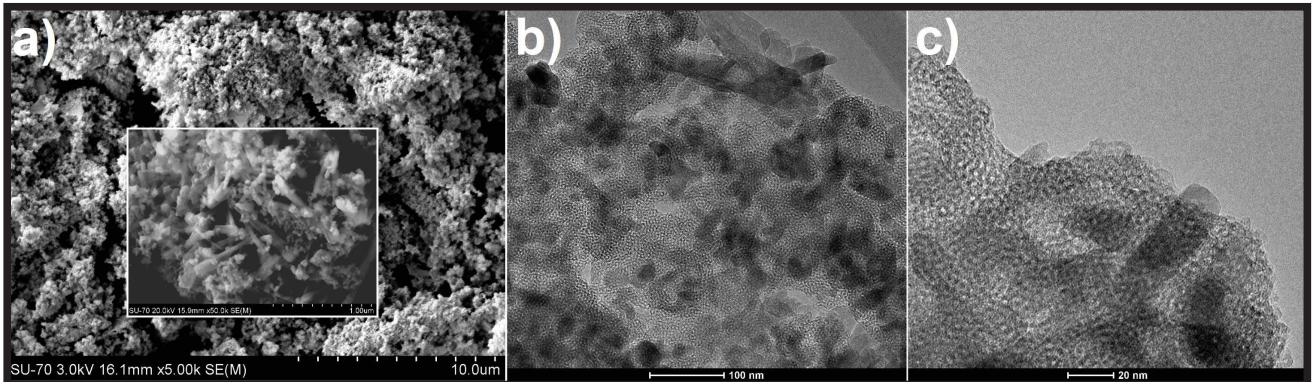


FIG. 2. The SEM (a) and TEM (b,c) micrographs of the obtained MSi-CaP-Cef composites.

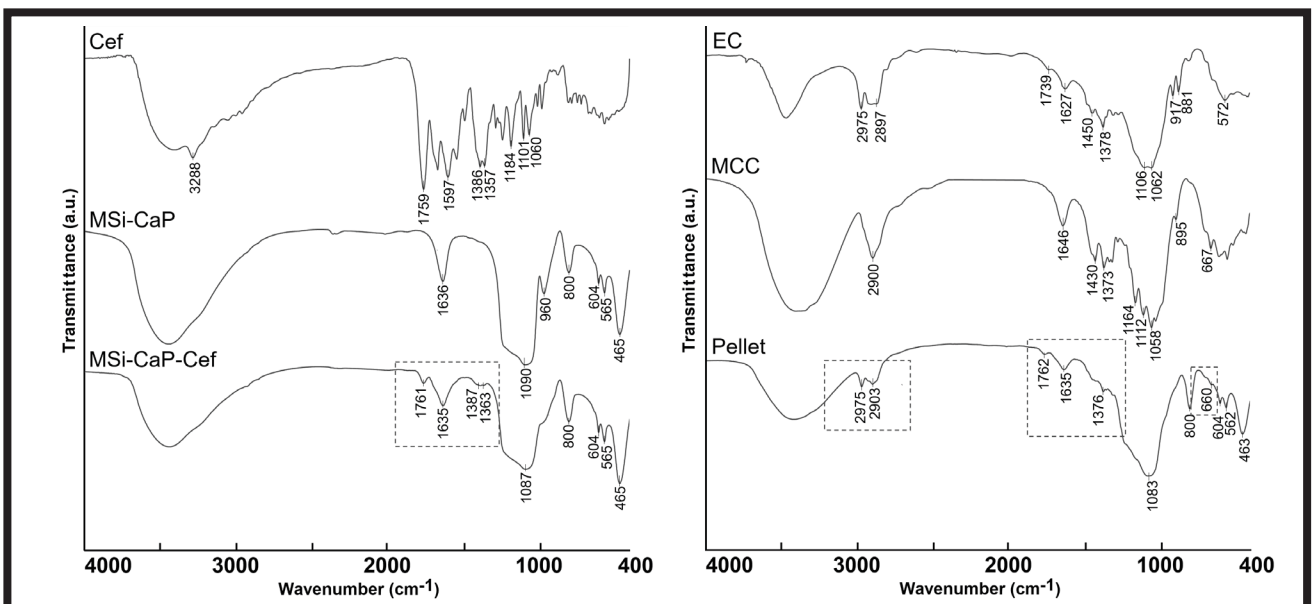


FIG. 3. The FTIR spectra of the MSi-CaP composite before and after Cef loading with the Cef reference sample (left) and the obtained pellet with the EC and MCC reference samples (right).

TABLE 1. The hardness and friability values of the MSi-CaP-Cef pellets.

Batch number	Force at 90% strain (g)	Mean \pm SD (g)	Friability (%)	Mean \pm SD (%)
1	58.3	59.0 \pm 4.3	2.1	2.3 \pm 0.3
2	64.5		2.7	
3	54.1		2.2	

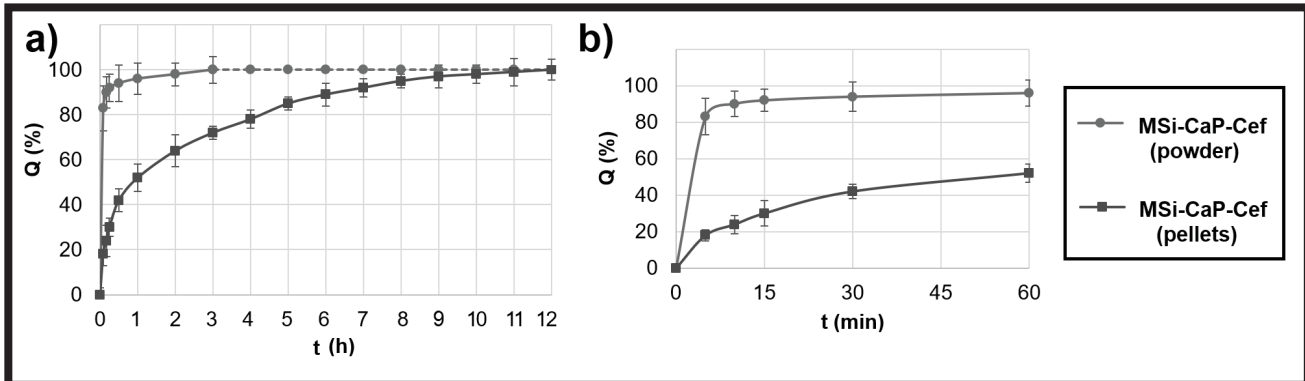


FIG. 4. The cefazolin release profiles (a) and burst release stage (b) of the MSi-CaP-Cef powders and pellets.

The hardness and friability of the CaP-MSi-Cef pellets are presented in TABLE 1. The mean force at 90% strain was 59.0 \pm 4.3 g, whereas the mean friability was 2.3 \pm 0.3. The similar results obtained for 3 independent batches confirmed the repeatability of the pelletization process. The obtained mechanical properties provided the pellets stability during the drug release studies and mineralization potential assay. The pellets did not disintegrate and stayed completely spherical after 60 days of incubation in SBF.

The drug release profiles of MSi-CaP-Cef composites in the form of powders and pellets are presented in FIG. 4. For the MSi-CaP-Cef powders the complete drug release was achieved after 3 h of studies (FIG. 4a) and it was preceded by high burst release – almost 90 \pm 6% of Cef was released during the first 15 min. It might suggest that chemical interactions between Cef molecules and the MSi-CaP composite surface were weak and did not have an important impact on the release profile. It should be noticed that both Cef molecules and silica surface are negatively charged under the performed conditions of drug release studies, so the electrostatic repulsion between those specimens might occur, increasing the burst stage [21]. Although the hydrogen bonding between Cef and the silica surface seems to be sufficient for drug loading, it cannot compensate for a relatively stronger electrostatic repulsion during the drug release. Thus, the high burst release is observed for the MSi-CaP-Cef powders. For the MSi-CaP-Cef composites shaped as pellets the complete drug release was observed after 12 h of studies (FIG. 4a) with a significantly slowed down burst stage (FIG. 4b) – the amount of Cef released after 15 min was reduced by 3 (from 90 \pm 6% to 32 \pm 5% for the powders and pellets, respectively). The prolonged release of the drug from the pellets can be explained as follows. The manufactured pellets had a much smaller surface area as compared to powders, thus the effective surface area available for water to dissolve the drug was significantly reduced. Moreover, the penetration of water into the pellets was impeded due to the presence of hydrophobic excipients: MCC and EC. The used excipients acted as a hydrophobic boundary which limited the access of water to drug molecules inside the matrix and consequently extended the diffusion path length [24].

The obtained pellets were characterized by a relatively fast (12 h) and complete CEF release as compared to other bone implants (>30 days) [25]. The fast drug release may ensure the high local concentration of antibiotics immediately after the orthopaedic surgery, thus reducing the dosage of parenteral antibiotics and the risk of side effects during the pharmacological treatment. Moreover, the complete drug release from the proposed MSi-CaP-Cef pellets seems to be an important feature of bone drug delivery systems preventing antibiotic resistance. In contrast, the commonly used bone cements are characterized by the incomplete and sustained release of loaded antibiotics causing the local sub-inhibitory concentrations in the infected bone that increase the risk of antibiotic resistance [26,27].

The SEM micrographs with corresponding EDX profiles for the MSi-CaP-Cef pellets before and after 60 days of mineralization potential assay in SBF are presented in FIG. 5. The primary pellets were characterized by a smooth surface composed of two domains: the MSi-CaP-Cef domain in the form of semi-spherical particles or rods (high Si, Ca, P content in EDX profile) and the MCC-EC domain in the form of elongated strands (high C, O content in EDX profile). The observed sulphur in the EDX profile no. 1 (FIG. 5, top) derived from the Cef molecules loaded into the MSi-CaP composites. After 60 days of mineralization assay, the surface of the pellets became rough with small (100-150 μ m length) cracks as a consequence of SBF penetration into the pellets matrix. The whole surface of pellets was covered by the needle-like and flower-shaped continuous layer. According to the EDX profile no. 2 (FIG. 5, bottom), the morphology of precipitate and our previous results [28], such a layer might be considered as the carbonated hydroxyapatite. However, it was also observed that some MCC-EC domains were not covered by the hydroxyapatite layer due to their weaker mineralization potential if compared to the MSi-CaP composite, which was confirmed by the EDX no. 1 (FIG. 5, bottom). The possible mechanism of carbonated hydroxyapatite formation on the pellets surface might be connected with the presence of calcium phosphate in the MSi-CaP composite.

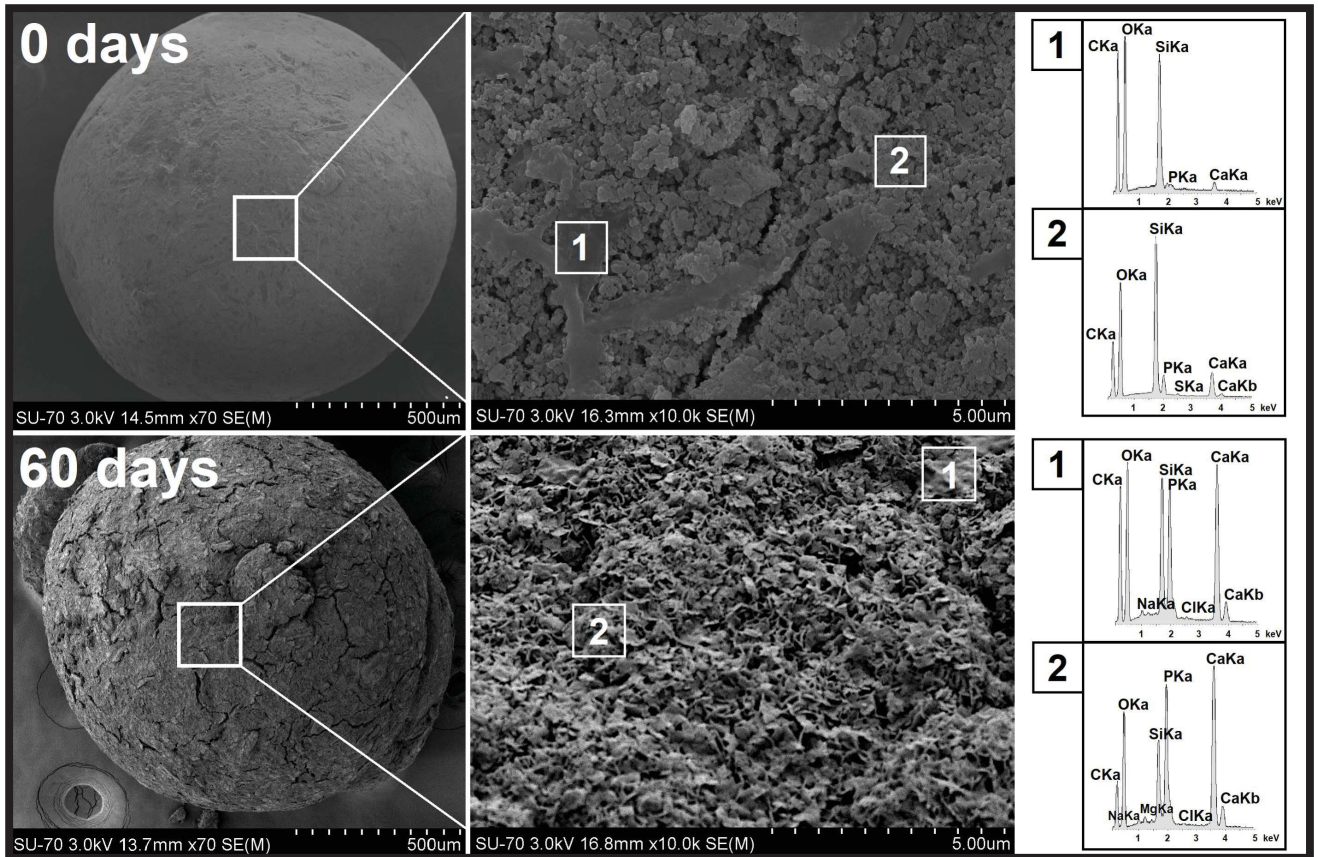


FIG. 5. The SEM micrographs with corresponding EDX profiles of the MSi-CaP-Cef pellets before and after 60 days of the mineralization assay in SBF.

Such a calcium phosphate may act as a metastable form which has partially dissolved in the SBF and precipitated on the surface of the pellets as the stable hydroxyapatite form. The precipitated hydroxyapatite nuclei absorb accessible calcium and phosphate ions from the SBF in order to form aggregates, clusters and continuous layers. The spreading of hydroxyapatite on the whole surface of the pellets was most probably promoted by the silanol groups of mesoporous silica which, in turn, facilitated the further formation of new hydroxyapatite nucleation centers. As it is presented in the EDX profile no. 2 (FIG. 5, bottom), the magnesium, sodium and carbonate ions were incorporated into the hydroxyapatite structure proving the dynamic nature of the apatite formation process. The Ca/P molar ratio of the formed hydroxyapatite was 1.71 (data not shown), thus similar to the human bone apatite.

The progressive formation of carbonated hydroxyapatite was also confirmed by the FTIR results (FIG. 6). The shift in the absorbance of the maximum peak from 1087 to 1092 cm^{-1} might be observed due to the increasing intensity of ν_3 (PO_4)³⁻ vibrational modes [29]. Moreover, after 60 days of the mineralization potential assay, the maximum absorbance peak divided into two: at 1092 and 1053 cm^{-1} , as a consequence of the increased P-O vibrations. The progressive increase of the peaks at 604, 562 cm^{-1} (ν_4 of P-O-P) in the function of the SBF incubation time was also observed. The relative increase in the bands' intensity in the 1450-1430 cm^{-1} region may be connected with the carbonates incorporated into the hydroxyapatite structure (ν_3 and C-O vibrational modes) [30].

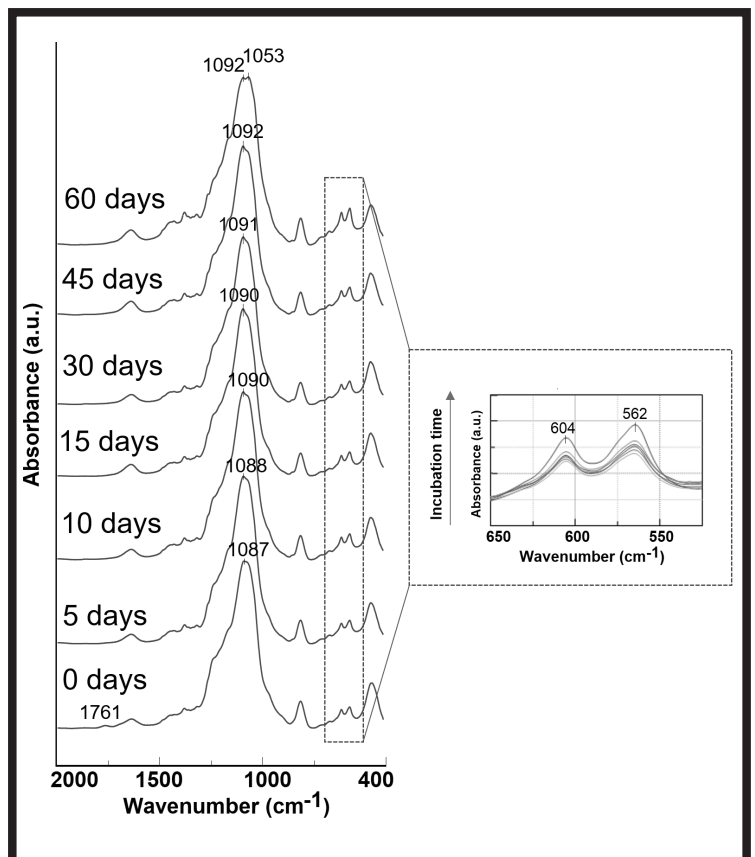


FIG. 6. The FTIR spectra of MSi-CaP-Cef pellets obtained during the mineralization potential assay in SBF.

Conclusions

The addition of calcium phosphate (CaP) precursors during the sol-gel process of mesoporous silica (MSi) synthesis allowed to obtain the biphasic MSi-CaP composites with preserved adsorption capacity. The cefazolin-loaded composites in the form of powders were suitable for the pelletization process, having added excipients. The obtained spherical granules (pellets) were characterized by the complete 12 h drug release and the surface hydroxyapatite formation after immersion in the simulated body fluid. The complete and relatively fast drug release from the pellets may support the pharmacological treatment of bacterial bone infections, immediately after the surgery. The obtained pellets require further studies (antimicrobial activity, cytotoxicity assay) to investigate their application potential in the fields of bone drug delivery systems.

Acknowledgments

This project was supported by the Polish National Science Centre (project OPUS 15 no. 2018/29/B/NZ7/00533) awarded to Magdalena Prokopowicz.

The study was supported by the project POWR.03.02.00-00-1026/17-00 co-financed by the European Union through the European Social Fund under the Operational Programme Knowledge Education Development 2014–2020.

References

- [1] M.C. Birt, D.W. Anderson, E. Bruce Toby, J. Wang: Osteomyelitis: Recent advances in pathophysiology and therapeutic strategies, *J. Orthop.* 14 (2017) 45–52.
- [2] N. Rao, B.H. Ziran, B.A. Lipsky: Treating Osteomyelitis: Antibiotics and Surgery, *Plast. Reconstr. Surg.* 127 (2011) 177S–187S.
- [3] J. Calhoun, M.M. Manring, M. Shirliff: Osteomyelitis of the long bones, *Semin. Plast. Surg.* 23 (2009) 059–072.
- [4] A.L.L. Lima, P.R. Oliveira, V.C. Carvalho, S. Cimerman, E. Savio: Recommendations for the treatment of osteomyelitis, *Brazilian J. Infect. Dis.* 18 (2014) 526–534.
- [5] M.R. Newman, D.S. Benoit: Local and targeted drug delivery for bone regeneration., *Curr. Opin. Biotechnol.* 40 (2016) 125–132.
- [6] I. Izquierdo-Barba, L. Ruiz-González, J.C. Doadrio, J.M. González-Calbet, M. Vallet-Regí: Tissue regeneration: A new property of mesoporous materials, *Solid State Sci.* 7 (2005) 983–989.
- [7] A. Oryan, S. Alidadi, A. Moshiri, N. Maffulli: Bone regenerative medicine: classic options, novel strategies, and future directions, *J. Orthop. Surg. Res.* 9 (2014) 18.
- [8] M. Vallet-Regí, I. Izquierdo-Barba, M. Colilla: Structure and functionalization of mesoporous bioceramics for bone tissue regeneration and local drug delivery, *Philos. Trans. R. Soc. A Math. Phys. Eng. Sci.* 370 (2012) 1400–1421.
- [9] C. Li, C. Jiang, Y. Deng, T. Li, N. Li, M. Peng, J. Wang: RhBMP-2 loaded 3D-printed mesoporous silica/calcium phosphate cement porous scaffolds with enhanced vascularization and osteogenesis properties, *Sci. Rep.* 7 (2017) 41331.
- [10] C. Bharti, U. Nagaich, A.K. Pal, N. Gulati: Mesoporous silica nanoparticles in target drug delivery system: A review., *Int. J. Pharm. Investig.* 5 (2015) 124–33.
- [11] J. Flynn, S. Mallen, E. Durack, P.M. O'Connor, S.P. Hudson: Mesoporous matrices for the delivery of the broad spectrum bacteriocin, nisin A, *J. Colloid Interface Sci.* 537 (2019) 396–406.
- [12] V.S. Kattimani, S. Kondaka, K.P. Lingamaneni: Hydroxyapatite—Present, and future in bone regeneration, *Bone Tissue Regen. Insights.* 7 (2016) 9–19.
- [13] D.K. Kim, S.J. Lee, T.H. Cho, P. Hui, M.S. Kwon, S.J. Hwang: Comparison of a synthetic bone substitute composed of carbonated apatite with an anorganic bovine xenograft in particulate forms in a canine maxillary augmentation model, *Clin. Oral Implants Res.* 21 (2010) 1334–1344.
- [14] S. Tang, B. Tian, Q.F. Ke, Z.A. Zhu, Y.P. Guo: Gentamicin-loaded carbonated hydroxyapatite coatings with hierarchically porous structures: drug delivery properties, bactericidal properties and biocompatibility, *RSC Adv.* 4 (2014) 41500–41509.
- [15] M. Prokopowicz, K. Czarnobaj, A. Szewczyk, W. Sawicki: Preparation and in vitro characterisation of bioactive mesoporous silica microparticles for drug delivery applications, *Mater. Sci. Eng. C.* 60 (2016) 7–18.
- [16] T. Kokubo, H. Takadama: How useful is SBF in predicting in vivo bone bioactivity?, *Biomaterials.* 27 (2006) 2907–2915.
- [17] J. Kecht, T. Bein: Oxidative removal of template molecules and organic functionalities in mesoporous silica nanoparticles by H₂O₂ treatment, *Microporous Mesoporous Mater.* 116 (2008) 123–130.
- [18] H. Chen, Y. Wang: Preparation of MCM-41 with high thermal stability and complementary textural porosity, *Ceram. Int.* 28 (2002) 541–547.
- [19] R. Al-Oweini, H. El-Rassy: Synthesis and characterization by FTIR spectroscopy of silica aerogels prepared using several Si(OR)₄ and R''Si(OR')₃ precursors, *J. Mol. Struct.* 919 (2009) 140–145.
- [20] H. Ye, X.Y. Liu, H. Hong: Characterization of sintered titanium/hydroxyapatite biocomposite using FTIR spectroscopy, *J. Mater. Sci. Mater. Med.* 20 (2009) 843–850.
- [21] A. Szewczyk, M. Prokopowicz, W. Sawicki, D. Majda, G. Walker: Aminopropyl-functionalized mesoporous silica SBA-15 as drug carrier for cefazolin: adsorption profiles, release studies, and mineralization potential, *Microporous Mesoporous Mater.* 274 (2019) 113–126.
- [22] J.M. Rosenholm, T. Czuryzkiewicz, F. Kleitz, J.B. Rosenholm, M. Lindén: On the nature of the Bronsted acidic groups on native and functionalized mesoporous siliceous SBA-15 as studied by benzylamine adsorption from solution, *Langmuir.* 23 (2007) 4315–4323.
- [23] M. Fan, D. Dai, B. Huang: Fourier Transform Infrared Spectroscopy for natural fibres, in: Salih Salih (Ed.), *Fourier Transform - Mater. Anal.*, 1st ed., InTech, 2012: pp. 45–68. <https://www.intechopen.com/books/fourier-transform-materials-analysis/fourier-transform-infrared-spectroscopy-for-natural-fibres> (accessed May 29, 2019).
- [24] M.A. Quadir, M.S. Rahman, M.Z. Karim, S. Akter, M.T. Bin Awkat, M.S. Reza: Evaluation of hydrophobic materials as matrices for controlled-release drug delivery. *Pak. J. Pharm. Sci.* 16 (2003) 17–28.
- [25] S.K. Nandi, S. Bandyopadhyay, P. Das, I. Samanta, P. Mukherjee, S. Roy, B. Kundu: Understanding osteomyelitis and its treatment through local drug delivery system, *Biotechnol. Adv.* 34 (2016) 1305–1317.
- [26] R. Dorati, A. DeTrizio, T. Modena, B. Conti, F. Benazzo, G. Gastaldi, I. Genta: Biodegradable scaffolds for bone regeneration combined with drug-delivery systems in osteomyelitis therapy, *Pharmaceuticals.* 10 (2017) 96.
- [27] E.A. Masters, R.P. Trombetta, K.L. de Mesy Bentley, B.F. Boyce, A.L. Gill, S.R. Gill, K. Nishitani, M. Ishikawa, Y. Morita, H. Ito, S.N. Bello-Irizarry, M. Ninomiya, J.D. Brodell, C.C. Lee, S.P. Hao, I. Oh, C. Xie, H.A. Awad, J.L. Daiss, J.R. Owen, S.L. Kates, E.M. Schwarz, G. Muthukrishnan: Evolving concepts in bone infection: redefining “biofilm”, “acute vs. chronic osteomyelitis”, “the immune proteome” and “local antibiotic therapy”, *Bone Res.* 7 (2019) 20.
- [28] M. Prokopowicz, J. Żeglinski, A. Szewczyk, A. Skwira, G. Walker: Surface-activated fibre-like SBA-15 as drug carriers for bone diseases, *AAPS PharmSciTech.* 20 (2019) 17.
- [29] G.M.L. Dalmónico, D.F. Silva, P.F. Franczak, N.H.A. Camargo, M.A. Rodríguez: Elaboration biphasic calcium phosphate nanostructured powders, *Boletín La Soc. Española Cerámica y Vidr.* 54 (2015) 37–43.
- [30] Y. Zheng, X. Liu, Y. Ma, T. Huo, Y. Li, C. Pei: Controlled synthesis of hydroxyapatite microspheres with hierarchical structure and high cell viability, *Mater. Lett.* 195 (2017) 18–21.